

Joint Rate and Fairness Improvement Based on Adaptive Weighted Graph Matrix for Uplink SCMA With Randomly Distributed Users

Maryam Cheraghy^{ID}, Wen Chen^{ID}, *Senior Member, IEEE*, Hongying Tang^{ID}, *Member, IEEE*,
Qingqing Wu^{ID}, *Member, IEEE*, and Jun Li^{ID}, *Senior Member, IEEE*

Abstract—Developing resource allocation algorithms for the uplink sparse code multiple access (SCMA) scheme to satisfy multiple objectives is challenging, especially where users are randomly distributed. In this paper, we aim to address this challenge by developing a joint resource allocation method as a multi-objective optimization (MO) problem to maximize the average sum rate and fairness among users as key and sub-key objectives, respectively. For this purpose, the exact analytical expressions for the average sum rate and users' individual rate are extracted based on an adaptive weighted graph matrix (AWGM). An AWGM matrix beneficially replaces the factor graph and the power allocation matrices to simplify the MO problem based on the asymmetric modified bipartite matching (AMBM) algorithm. The power allocation strategy is utilized during the optimal resource assignment process using the AMBM algorithm. After the AMBM process, we propose a low-complexity four-step algorithm to obtain the AWGM. The simulation results show that our proposed method can compromise and improve the multiple objectives' performance and guarantees a stable range of network performance at different times.

Index Terms—Sparse code multiple access, multi-objective optimization, asymmetric bipartite matching, randomly deployed users, resource allocation.

I. INTRODUCTION

THE service quality of higher throughput, lower latency and massive connectivity can be enabled by exploiting efficient spectrum usage in the fifth generation (5G) wireless communication systems [1], [2]. The limited accessibility to the spectrum has led to severe challenges [3],

which can be overcome through sparse code multiple access (SCMA) [4]. SCMA is a non-orthogonal multiple access technology, allowing multiple users to share the same resource block (RB) while providing an acceptable decoding complexity [5], [6]. In [7] and [8], the authors proposed an approach to design a set of SCMA codebooks with the joint optimization of multi-dimensional modulation and low-density spreading, which allows multiple users to share the same RB with tolerable decoding complexity. In SCMA, instead of simple repetition of quadrature amplitude modulation symbols in low-density systems, coded bits are directly mapped into multi-dimensional sparse codewords selected from layer-specific SCMA codebooks [9]. The joint optimization of both the factor graph matrix and the modulation constellation control the SCMA system performance.

A codebook construction based on a connection of factor graphs of several RBs, known as the extended factor graph, was presented in [10] to achieve diversity gain. In [11], the authors proposed a scheme of the factor graph matrix facing large-scale customers, where a quasi-cyclic property with shifting was introduced in the construction of the factor graph matrix. The dynamic factor graph was implemented in [12] by comparing all factor graph edges' belief values and selecting the edges with better performance for the message passing algorithm (MPA). The factor graph matrix was designed in [13], with the assumption of known distances between users and base stations (BS), which maximizes the average sum rate of SCMA systems. However, the power allocation was not considered, while the codebook design using rotated constellation was developed in [14]. So in [10]–[13], the factor graph matrix was presented, whereas the constellation design is the goal of [14]. A single design factor simplified the codebook design procedure by a decimal signature matrix replacing the two mentioned design factors [15].

A. Related Works

The average sum rate has an essential role in the performance, and the SCMA factor graph matrix is useful in both the system transmission rate and decoding complexity. In [16], a capacity-based codebook design scheme for SCMA was proposed by calculating the derivation of the achievable rate formula, but the resource assignment was not considered. In [17], a weighted rate and energy maximization

Manuscript received June 30, 2020; revised November 10, 2020 and February 2, 2021; accepted February 3, 2021. Date of publication February 11, 2021; date of current version May 18, 2021. This work is supported by National Key Project 2018YFB1801102 and 2020YFB1807700, Shanghai Fundamental Project 20JC1416502, and NSFC 62071296 and 61872184. The associate editor coordinating the review of this article and approving it for publication was D. Niyato. (*Corresponding author: Wen Chen.*)

Maryam Cheraghy and Wen Chen are with the SICS, Department of Electronic Engineering, Shanghai Jiao Tong University, Shanghai 200240, China (e-mail: maryamcheraghy71@sjtu.edu.cn; wenchen@sjtu.edu.cn).

Hongying Tang is with the Institute of Microsystems and Information Technology, Chinese Academy of Sciences, Shanghai 200050, China (e-mail: tanghy@mail.sim.ac.cn).

Qingqing Wu is with the Department of Electrical and Computer Engineering, University of Macau, Taipa 117576, China (e-mail: qingqingwu@um.edu.mo).

Jun Li is with the School of Electronic and Optical Engineering, Nanjing University of Science and Technology, Nanjing 210094, China (e-mail: jun.li@njust.edu.cn).

Color versions of one or more figures in this article are available at <https://doi.org/10.1109/TCOMM.2021.3058529>.

Digital Object Identifier 10.1109/TCOMM.2021.3058529

0090-6778 © 2021 IEEE. Personal use is permitted, but republication/redistribution requires IEEE permission.

See <https://www.ieee.org/publications/rights/index.html> for more information.

problem by jointly considering power allocation, codebook assignment, and power splitting for the SCMA networks was formulated. In [18], the resource allocation problem of the single-cell SCMA network was developed as an optimization problem to maximize the system capacity. A suboptimal algorithm was proposed by separating the power allocation and codebook assignment. In [19], a power allocation algorithm was presented to maximize the sum capacity of the system, and the Lagrange dual decomposition method was employed to solve the non-convex optimization problem. However, in [17]–[19], the downlink scenario was investigated without considering the users' fairness optimization problem.

In [20], the capacity region for uplink SCMA systems was analyzed, based on which the common and individual outage probability regions are calculated. However, the analytical expression for users' individual rates and the resource assignment optimization problem, i.e., selecting the optimal factor graph matrix and the fairness optimization, were not considered. In [21], two new iterative algorithms were proposed to jointly optimize the subcarrier assignment and the transmitted power per subcarrier for the uplink SCMA systems by applying a variant of block successive upper-bound minimization (BSUM) scheme. The sum rate and the fairness of the network were maximized by Max-SR and Max-Min algorithms. However, two objectives as two performance metrics were optimized separately. There was no trade-off between these two objectives, and multi-objective (MO) optimization was not utilized either. Since different forms of technical preparation metrics are presented in 5G systems, and these multiple objectives are conjoined together and often inconsistent, one objective improvement usually leads to the deterioration of other objectives.

It is also worth noting that none of the mentioned studies has analyzed the users' random distances. The performance analysis of SCMA with randomly deployed users is limited in [22]–[24]. In [22], an analytical expression was derived for the average sum rate of uplink SCMA systems in a hexagon cell with uniformly distributed users. But the resource allocation problem and an analytical expression for users' individual rates were not considered. According to this scenario in [24], pairwise error probability was analyzed and evaluated. The area spectral efficiency and success probability, while taking into account the impact of mutual interference and the codeword structure, were formulated for a large-scale spatial random SCMA wireless network in [23]. However, the resource allocation optimization problem was not considered. To achieve the 5G vision that appropriately manages the presence and trade-off between multiple targets, we need to establish resource allocation strategies for the pervasive deployment of high throughput SCMA networks. It is vital to calculate a good factor graph matrix and power allocation coefficients to improve the average sum rate in SCMA systems, especially when the signal to noise ratios (SNRs) of users are entirely different. Therefore, considering the randomly deployed users to evaluate the SCMA network performance metrics is a crucial affair, and in this term, per-user performance improvement will be significant.

Graph theory is an efficient method for resource allocation design in wireless networks. In [25], to solve the mixed-integer non-linear program optimization problem with a non-convex feasibility set, the original problem was decomposed into two sub-problems: codebook allocation based on the bipartite graph theory, and power allocation by using geometric water filling approach. But downlink energy efficiency (EE) optimization problem of SCMA system was considered, and the codebook allocation according to the maximum normalized rate was done. To solve the assignment problem, an algorithm forming a maximum weight perfect matching in a bipartite graph was investigated by the Kuhn-Munkres (KM) method [26]. KM algorithm is a suitable method that can find the best solution for the maximum weighted sum and assignment. In [27], a user grouping method was presented to maximize the system capacity by employing the KM method to solve the weighted bipartite matching problem. The optimal matching problem was investigated in [28] based on the bipartite graph and considering the mutual interference constraints to maximize sum rates under transmit power and outage constraints. In [29], a weighted bipartite matching approach was used to solve the interference minimization problem. Reference [30] employs the successive interference cancellation algorithm to estimate each user's channel response based on the bipartite graph. Codebook assignment of device-to-device communication in uplink SCMA was considered in [31] by using the maximum weighted bipartite matching method. It is based on the KM algorithm to find the optimal solution efficiently and sum-rate maximization.

B. Contributions

In this paper, we aim to maximize the average sum rate as a key objective while satisfying all users' fairness as a sub-key objective for an uplink SCMA network, where the users are randomly distributed in a disk-shaped cell. We investigate an approach based on graph theory to solve resource allocation optimization problems. For this purpose, the adaptive weighted graph matrix (AWGM) is presented, which is the combination of power allocation coefficients and factor graph matrix. Firstly, we formulate this problem by AWGM. Then analytical expressions for the average sum rate and users' individual rate of the uplink SCMA scheme are derived. We solve the dual-objective resource allocation problem for the SCMA scheme by the asymmetric modified bipartite matching (AMBM) algorithm [32] and a low-complexity four-step algorithm. For the average sum rate maximization, the KM algorithm is utilized for each modified bipartite graph obtained by removing one edge at a time until no edge remains in the graph, and AMBM chooses the optimal matching to satisfy system requirements [32]. To determine which edge should be removed, we need to individually define the edge that has the least contribution to the fairness optimization. Although the AMBM algorithm based on the KM method provides an optimal assignment solution, but cannot be extended to an SCMA system directly. The reason is that the SCMA scheme has additional constraints, i.e., the number of RBs required by users for concurrent transmission and the number

of users each RB can support. Thus, we propose a four-step algorithm combined with the mentioned method and then extract AWGM. Therefore, the AWGM for both key and sub-key objectives determines the power allocation coefficients and gives the optimal resource assignment matrix. This paper assumes that the BS is located in the center of the disk-shaped cell based on the perfect channel state information. The main contributions of this paper are listed as follows.

- We derive the analytical expressions of the average sum rate based on the compilation of the power allocation coefficients and factor graph matrix, i.e., AWGM in the uplink SCMA system with randomly deployed users in the disk-shaped cell. The exact analytical expression for the individual rates based on the average sum rate is presented by using the joint moment generation function (MGF) method [33].

- For the first time, we formulate the MO method to solve the SCMA joint resource allocation problem with low computational complexity and adaptively select a proper solution. This method provides a useful tool to balance between the average sum rate and fairness among users.

- A power allocation strategy for improving the objectives performance is used in the optimal resource assignment by using the AMBM method. A single design matrix beneficially replaces the factor graph matrix and power allocation matrix of the joint problem by designing the AWGM, which simplifies our MO joint resource allocation. Moreover, a four-step algorithm is proposed to tackle the generalization problem of AMBM for the SCMA scheme.

- Finally, we compare our proposed method with the other three SCMA algorithms. The first two algorithms, i.e., Max-SR and Max-Min schemes, are based on the BSUM method [21]. The third algorithm, named TA-PA, is based on the throughput-aware assignment (TA) scheme in [25] and the power allocation (PA) method in [9]. The simulation results show that our proposed method can compromise two objectives while guaranteeing a stable range of network performance rather than others.

The rest of the paper is organized as follows. Section II introduces the SCMA system model. Section III focuses on the AWGM, average sum rate, and individual rate. Section IV describes the MO resource allocation based on AMBM. The theoretical analysis is confirmed by simulations in Section V. Finally, conclusions are made in Section VI.

C. Notations

Lowercase and uppercase bold letters denote vectors and matrices, respectively. We use $[\cdot]^T$, $[\cdot]^*$, $[\cdot]^H$, and $\|\cdot\|$ to denote transpose, conjugate transpose, hermitian conjugate, and Euclidean norm, respectively, while $\|\cdot\|_0$ represents the number of non-zero elements of the row or column vectors of the matrix. $\text{diag}(\mathbf{h}_j)$ denotes the diagonal matrix whose k th diagonal entry is $h_j[k]$. The expectation operator is denoted by $\mathbf{E}\{\cdot\}$, and the notation $\det(\cdot)$ denotes the matrix determinant operation, while \mathbf{I}_K is the $K \times K$ identity matrix.

II. SYSTEM MODEL

We consider a system consisting of one BS and J users spreading over K orthogonal RBs. As shown in Fig. 1, the BS

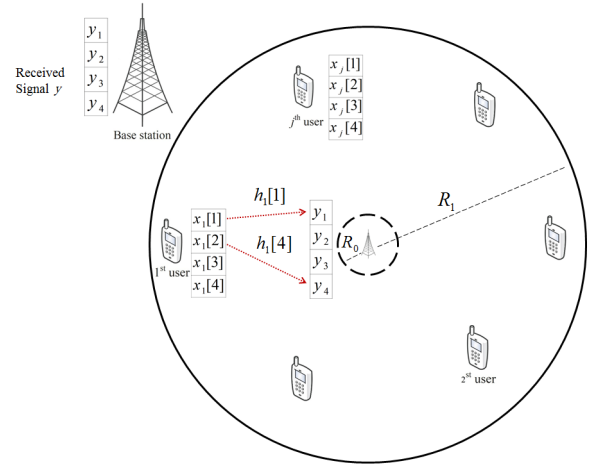


Fig. 1. The SCMA network with randomly distributed users in the disk-shaped cell. R_0 and R_1 show the minimum and maximum communication distances of users from BS, respectively.

is located at the center of the disk-shaped cell. The users with a single antenna are uniformly distributed within the cell and the overloading factor of the system is $\frac{J}{K}$. Suppose that d_k is the number of users supported by each RB, i.e., $d_k = \frac{JN}{K}$ [8], and N denotes the number of RBs that can be used by each user. Furthermore, the length of the codeword is K .

The transmitted symbol of the j th user is a K -dimensional symbol denoted by $\mathbf{x}_j = [x_j[1], \dots, x_j[K]]^T$ with N non-zero elements. The channel vector between the j th user and all RBs is $\mathbf{h}_j = [h_j[1], \dots, h_j[K]]^T$, where $h_j[k] = g_j[k]d_j^{-\frac{\alpha}{2}}$, $g_j[k] \sim \mathcal{CN}(0, 1)$ represents a Rayleigh fading coefficient. d_j represents the distance from the j th user and BS, and α is the path loss exponent. After multiplex layers, the received signal $\mathbf{y} = [y_1, \dots, y_K]^T$ can be expressed as

$$\begin{aligned} \mathbf{y} &= \sum_{j=1}^J \sqrt{E_t} \text{diag}(\mathbf{w}_j) \text{diag}(\mathbf{h}_j) \mathbf{x}_j + \mathbf{n} \\ &= \sum_{j=1}^J \sqrt{E_t} \text{diag}(\mathbf{h}_j) \mathbf{X}_j + \mathbf{n}, \end{aligned} \quad (1)$$

where $\mathbf{n} \sim \mathcal{CN}(0, N_0 \mathbf{I})$ and E_t are the complex Gaussian noise and the total transmitting power of each user, respectively. The power allocation coefficient vector of j th user is $\mathbf{w}_j = [\sqrt{\omega_j[1]}, \dots, \sqrt{\omega_j[K]}]^T$, where if $x_j[k] = 0$, then $\omega_j[k] = 0$ and if $x_j[k] \neq 0$ then $\omega_j[k] \neq 0$. $\mathbf{X}_j = \text{diag}(\mathbf{w}_j) \mathbf{x}_j$, and $\mathbf{E}\{(x_j[k])(x_j[k])^*\} = 1$; therefore, the auto-correlation matrix is diagonal, i.e., $\mathbf{E}\{\mathbf{X}_j \mathbf{X}_j^H\} = \text{diag}(\omega_j[1], \dots, \omega_j[K])$.

The path loss in terms of d_j is expressed as follows [34]

$$d_j^{-\alpha} = \begin{cases} d_j^{-\alpha}, & R_0 < d_j \leq R_1, \\ R_0^{-\alpha}, & \text{otherwise,} \end{cases} \quad (2)$$

where parameters R_0 and R_1 denote the minimum and maximum user link distances, respectively. The probability distributed function (PDF) for the link distance from the guard zone R_0 to the endpoint of R_1 is as follows [23]

$$f_D(d) = \frac{2d}{(R_1^2 - R_0^2)}. \quad (3)$$

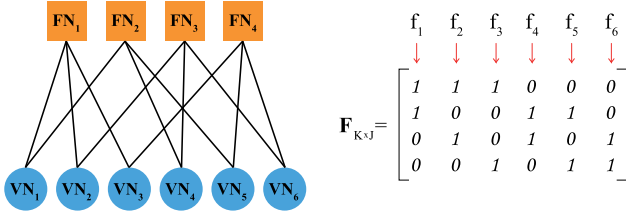


Fig. 2. Example of factor graph representation with $K = 4$, $J = 6$, $N = 2$ and $d_f = 3$.

III. AWGM, AVERAGE SUM RATE AND INDIVIDUAL RATE

To better understand the AWGM, a brief review is provided regarding a factor graph representation in most of the literature and it is compared with the AWGM. MPA is an effective method based on a factor graph for estimating the input signals. In other words, MPA messages lead to the calculation of probability distribution for \mathbf{x}_j , and the updating process of these messages is influenced by the constraints applied by the factor graph. At the receiving end, the MPA detector on the underlying factor graph is utilized for multi-user detection [5]–[7].

In most conventional SCMA systems, the decision about the connections between the users and RBs is performed by factor graph matrix $\mathbf{F}_{K \times J}$ [5], [6]. $\mathbf{f}_j = [f_j[1], \dots, f_j[K]]^T$ denotes the j th column of $\mathbf{F}_{K \times J}$, where $f_j[k]$ is the RB index with $f_j[k] = 1$, if $x_j[k] \neq 0$, and $f_j[k] = 0$, if $x_j[k] = 0$ [13]. Fig. 2 shows the factor graph matrix $\mathbf{F}_{K \times J}$ by assuming $N = 2$ and $d_k = 3$, where the variable nodes (VNs) and the functional nodes (FNs) denote the user nodes and RB nodes, respectively. For instance, the signal received by BS at RB1 and RB3 can be written as

$$y_1 = \sqrt{E_t}(h_1[1]x_1[1] + h_2[1]x_2[1] + h_3[1]x_3[1]) + n_1,$$

and

$$y_3 = \sqrt{E_t}(h_2[3]x_2[3] + h_4[3]x_4[3] + h_6[3]x_6[3]) + n_3.$$

The AWGM, represented by \mathbf{W} , involves the entries playing the RB assignment roles and the weight coefficients of power allocation. The unknown entries of AWGM are determined according to the objectives of the problem. The AWGM can be easily adjusted to the targets and satisfies the optimization problem conditions in IV.

The AWGM is defined as

$$\mathbf{W} = \begin{bmatrix} \sqrt{\omega_1[1]} & \dots & \sqrt{\omega_J[1]} \\ \vdots & \ddots & \vdots \\ \sqrt{\omega_1[K]} & \dots & \sqrt{\omega_J[K]} \end{bmatrix}. \quad (4)$$

For the factor graph shown in Fig. 2, the AWGM-based received symbol at RB1 is given by

$$y_1 = \sqrt{\omega_1[1]}h_1[1]x_1[1] + \sqrt{\omega_2[1]}h_2[1]x_2[1] + \sqrt{\omega_3[1]}h_3[1]x_3[1] + n_1,$$

where $E_t = 1$ is set for simplicity. Hence, for Fig. 2, \mathbf{W} can be simplified as

$$\mathbf{W} = \begin{bmatrix} \sqrt{\omega_1[1]} & \sqrt{\omega_2[1]} & \sqrt{\omega_3[1]} & 0 & 0 & 0 \\ \sqrt{\omega_1[2]} & 0 & 0 & \sqrt{\omega_4[2]} & \sqrt{\omega_5[2]} & 0 \\ 0 & \sqrt{\omega_2[3]} & 0 & \sqrt{\omega_4[3]} & 0 & \sqrt{\omega_6[3]} \\ 0 & 0 & \sqrt{\omega_3[4]} & 0 & \sqrt{\omega_5[4]} & \sqrt{\omega_6[4]} \end{bmatrix}. \quad (5)$$

As a new resource allocation scheme for the uplink SCMA system, we need to develop techniques to improve the objectives and compromise between them. This paper attempts to design the AWGM to increase the average sum rate and user fairness while balancing two objectives when Rayleigh fading channel conditions are assumed and users are located at random distances from the BS. In an SCMA system, resource assignment and power allocation are crucial for improving network performance.

A. Average Sum Rate

According to [35, eq. (2.14-15)] and [36], the capacity region considering the number of non-zero identical elements for all the users in the uplink SCMA network is expressed as follows

$$\sum_{j=1}^J R^j \leq \mathbf{E}_{\mathbf{h}} \left\{ \log \det \left(\mathbf{I}_{K \times K} + \frac{E_t}{N} \sum_{j=1}^J \text{diag}(\mathbf{h}_j) \mathbf{E} \{ \mathbf{X}_j \mathbf{X}_j^H \} \left(\text{diag}(\mathbf{h}_j) \right)^H \right) \right\}, \quad (6)$$

where R^j , for $j = 1, \dots, J$, is the achievable rate of the j th user, and $\mathbf{E}_{\mathbf{h}}$ is the expectation with respect to $\mathbf{h} = (\mathbf{h}_1, \dots, \mathbf{h}_J)$. Then the sum rate R_{SCMA} can be obtained by the following theorem.

Theorem 1: Under the normalized noise variance, the upper bound for average sum rate of SCMA network for all users with random distance to cell center can be given as

$$\begin{aligned} R_{SCMA} &\triangleq \sum_{j=1}^J R^j 2 \\ &= \mathbf{E} \left\{ \sum_{k=1}^K \log \left(1 + \frac{E_t}{N} \sum_{j=1}^J \omega_j[k] |g_j[k]|^2 d_j^{-\alpha} \right) \right\} \\ &\triangleq \mathbf{E} \left\{ \sum_{k=1}^K \log \left(1 + \frac{E_t}{N} \sum_{j=1}^J \mu_j \right) \right\}, \end{aligned} \quad (7)$$

where $\mu_j = \omega_j[k] |g_j[k]|^2 d_j^{-\alpha}$.

Proof: See Appendix A.

Since (6) and (7) are independent of signal codewords structure \mathbf{x}_j because $\mathbf{E} \{ \mathbf{x}_j \mathbf{x}_j^H \} = \mathbf{I}_{K \times K}$. Using $\ln(1+z) = \int_0^\infty \frac{e^{-s}}{s} (1 - e^{-sz}) ds$ [37] and $\mathbf{E} \{ e^{-sz} \} = \mathcal{L}_z(s)$, where \mathcal{L} shows Laplace transformation, we have

$$\begin{aligned} R_{SCMA} &= \frac{1}{\ln 2} \sum_{k=1}^K \int_{s=0}^{\infty} \frac{e^{-s}}{s} \left(1 - \prod_{j=1}^J \mathcal{L}_{\mu_j} \left(s \frac{E_t}{N} \right) \right) ds, \end{aligned} \quad (8)$$

where

$$\begin{aligned}\mathcal{L}_{\mu_j} \left(s \frac{E_t}{N} \right) &= \mathbf{E} \left\{ e^{-\frac{sE_t}{N} \mu_j} \right\} \\ &= \int_0^\infty e^{-\frac{sE_t}{N} \mu_j} f_{\mu_j}(\mu) d\mu,\end{aligned}\quad (9)$$

and $f_{\mu_j}(\mu)$ is the PDF of μ_j . Since $\mu_j = \omega_j[k] |g_j[k]|^2 d_j^{-\alpha}$, we need to calculate the PDF of two independent random variables of $V_j = \omega_j[k] |g_j[k]|^2$ and $d_j^{-\alpha}$. Since $g_j[k]$ is a Rayleigh fading channel gain, thus V_j is an exponential random variable with expectation $\omega_j[k]$ and the following PDF is given by

$$f_{V_j}(v) = \frac{1}{\omega_j[k]} e^{-\frac{v}{\omega_j[k]}}. \quad (10)$$

Employing (2), (3), and (10), $f_{\mu_j}(\mu)$ is given as

$$f_{\mu_j}(\mu) = \frac{2}{(R_1^2 - R_0^2)} \int_{R_0}^{R_1} x^{\alpha+1} f_{V_j}(x^\alpha \mu) dx. \quad (11)$$

Therefore, we can further calculate the sum rate of an uplink SCMA system by the following theorem.

Theorem 2: An analytical expression of the average sum rate of uplink SCMA for the disk-shaped cell is given by

$$\begin{aligned}R_{SCMA} &= \frac{1}{\ln 2} \sum_{k=1}^K \int_0^\infty \frac{e^{-s}}{s} \left(1 - \prod_{j=1}^J \left(\frac{2}{R_1^2 - R_0^2} \right) \times \right. \\ &\quad \left. \frac{N}{sE_t \omega_j[k] (\alpha + 2)} \times \left(x^{\alpha+2} \tilde{H} \left(\frac{-Nx^\alpha}{sE_t \omega_j[k]} \right) \Big|_{R_0}^{R_1} \right) \right) ds,\end{aligned}\quad (12)$$

and

$$\begin{aligned}\tilde{H} \left(\frac{-Nx^\alpha}{sE_t \omega_j[k]} \right) &\triangleq {}_2F_1 \left(1, 1 + \frac{2}{\alpha}, 2 + \frac{2}{\alpha}, - \left(\frac{N}{sE_t \omega_j[k]} \right) x^\alpha \right).\end{aligned}\quad (13)$$

where ${}_2F_1$ is the Gauss hyper-geometric function, and \tilde{H} is the simple representation of ${}_2F_1$ [38].

Proof: See Appendix B.

B. Individual Rate

Before presenting the individual rate of each user, two points should be noted here: Firstly, as previously described, we have $\mathbf{E} \{ \mathbf{x}_j \mathbf{x}_j^H \} = \mathbf{I}_{K \times K}$, and the individual rate of a user allocated to a specific RB is influenced by some other users using the same RB. Therefore, $x_j[k]$ is not crucial for a user's individual rate. Secondly, the j th user allocates merely one element of its N non-zero elements to one RB. Meanwhile, this RB supports the other users that may cause interference to the j th user in the corresponding RB, while these interfering users are unknown. Hence the individual rate of the j th user over RB k can be derived by the following theorem.

Theorem 3: Suppose that the k th RB is assigned to the j th user. Using (7), the individual rate of j th user in the k th RB is

$$R_k^j = \mathbf{E} \left\{ \log \left(1 + \frac{\omega_j[k] |g_j[k]|^2 d_j^{-\alpha}}{\sum_{t=1, t \neq j}^J \omega_t[k] |g_t[k]|^2 d_t^{-\alpha}} \right) \right\}. \quad (14)$$

Proof: See Appendix C.

It might be a mistake to suppose that (14) can be solved using the following formula.

$$\begin{aligned}\mathbf{E}_{g,d} \left\{ \log \left(1 + \frac{\mu_j}{\chi_k} \right) \right\} &= \mathbf{E}_d \left\{ \int_0^\infty \frac{1}{s} (1 - \mathbf{E}_g \{ e^{-s\mu_j} \}) \mathbf{E}_g \{ e^{-s\chi_k} \} ds \right\},\end{aligned}$$

where

$$\chi_k = \sum_{t=1, t \neq j}^J (\omega_t[k] |g_t[k]|^2 d_t^{-\alpha}).$$

It provides a closed-form in terms of the weight elements, R_1 and R_0 . Nevertheless, this method is inappropriate for (14) because dependent random functions have the same distributions in numerator and denominator. Hence, using the MGF method [33], the exact closed-form representation of R_k^j can be derived as follows

$$R_k^j = \mathbf{E}_d \left\{ \sum_{e=1}^E \sigma_e \frac{M_{\chi_k}(\beta_e) - M_{\mu_j, \chi_k}(\beta_e)}{\beta_e} \right\}, \quad (15)$$

where

$$\begin{aligned}M_{\mu_j, \chi_k}(s) &= \frac{1}{1 + \frac{d_j^{-\alpha}}{\omega_j[k]} s} \prod_{t=1, t \neq j}^J \frac{1}{1 + \frac{d_t^{-\alpha}}{\omega_t[k]} \frac{s}{t} + \frac{d_t^{-\alpha}}{\omega_t[k]} \frac{(t-1)s}{t}},\end{aligned}\quad (16)$$

and

$$M_{\chi_k}(s) = \prod_{t=1, t \neq j}^J \frac{1}{1 + \left(\frac{t-1}{t} \right) \frac{d_t^{-\alpha}}{\omega_t[k]} s}. \quad (17)$$

σ_e and β_e are sample points of the Laguerre polynomial [38] and

$$\mathbf{E} \{ d_j^{-\alpha} \} = \frac{2(R_0^{2-\alpha} - R_1^{2-\alpha})}{(\alpha - 2)(R_1^2 - R_0^2)}.$$

Each N non-zero element of \mathbf{x}_j is separately allocated to an RB considering the improvement of performance metrics and balancing the whole SCMA system performance. Our attempts involve calculating $\omega_j[k]$ in achieving the highest amount of both average sum rate and fairness among users, leading to extraction of AWGM. Derivation of $\omega_j[k]$ through $\max R_{SCMA}$ is intractable. In the next section, AWGM elements are derived by using the AMBM.

IV. SCMA MULTI-OBJECTIVE JOINT RESOURCE ALLOCATION

In this section, we formulate the joint resource allocation problem as a dual-objective optimization problem whose purpose is to maximize the average sum rate and fairness among users as key and sub-key objectives, respectively. For this purpose, we use the variation of power allocation coefficients for improving the objective performance during the optimal resource assignment process based on the AMBM method. Applying AWGM simplifies our procedure compared to the other methods, which even utilize assignment and power allocation matrices separately to solve a joint resource allocation

problem [9], [17], [18], [20], [21], [25]. Considering that, these two matrices are beneficially replaced by a single design matrix, i.e., AWGM, which is simultaneously used to optimize two objectives. \mathcal{R}_1 and \mathcal{R}_2 are key and sub-key objectives, respectively. AWGM is determined by achieving the maximum of both objectives according to the AMBM method through all possible states for matching defined in Section IV-A in detail. R_k^j and $\omega_j[k]$ denote the weights of edges and weight elements according to the individual rate. Without loss of generality, the representation of the MO problem considering two optimization targets is $\max_{\mathbf{W}}(\mathcal{R}(\mathbf{W})) = (\mathcal{R}_1(\mathbf{W}), \mathcal{R}_2(\mathbf{W}))$, and it is modified according to the method of [32] and is shown as follows

$$\begin{aligned} \mathbf{P1} : \max_{\mathbf{W}} \mathcal{R}_1(\mathbf{W}) &= \sum_{j=1}^J \sum_{k=1}^K R_k^j, \\ \text{s.t. } \mathbf{C1} : \mathcal{R}_2(\mathbf{W}) &\leq \epsilon, \\ \mathbf{C2} : \sum_{k=1}^K \omega_j[k] &\leq 1, \forall j \in \mathcal{J}, \\ \mathbf{C3} : \|\mathbf{W}_k^{\text{row}}\|_0 &= d_k, k \in \mathcal{K}, \\ \mathbf{C4} : \|\mathbf{W}_j^{\text{col}}\|_0 &= N, \forall j \in \mathcal{J}, \\ \mathbf{C5} : \omega_j[k] &\geq 0, \forall j \in \mathcal{J}, \forall k \in \mathcal{K}, \end{aligned} \quad (18)$$

In (18), \mathcal{R}_1 is the average sum rate according to (14), and \mathcal{R}_2 in C1 is the Jain's fairness index (JFI) [39].

$$\mathcal{R}_2(\mathbf{W}) = \text{JFI}(\mathbf{W}) = \frac{\left(\sum_{j=1}^J \sum_{k=1}^K R_k^j \right)^2}{J \left(\sum_{j=1}^J \left(\sum_{k=1}^K R_k^j \right)^2 \right)} \leq \epsilon. \quad (19)$$

The role of \mathcal{R}_2 with a constraint ϵ will be explained in part A of this Section. The conditions of the power allocation coefficients applied on the weight elements are represented by C2 and C5, where \mathcal{J} is the set of users. In C3 and C4, $\|\mathbf{W}_k^{\text{row}}\|_0$ and $\|\mathbf{W}_j^{\text{col}}\|_0$ represent the number of non-zero elements in the k th row and j th column of the AWGM, respectively. Where \mathcal{K} , $\mathbf{W}_k^{\text{row}}$, and $\mathbf{W}_j^{\text{col}}$ show the set of RBs, the k th row, and the j th column of \mathbf{W} , respectively. According to (14), the objective function of **P1** is non-convex. To simplify this, let us consider the objective function in terms of the achievable rate per user.

$$\begin{aligned} \mathbf{P2} : \max_{\mathbf{W}} \mathcal{R}_1(\mathbf{W}) &= \sum_{j=1}^J R^j, \\ \text{s.t. } \mathbf{C1}, \mathbf{C2}, \mathbf{C3}, \mathbf{C4}, \mathbf{C5}. \end{aligned} \quad (20)$$

By Theorem 1, the objective function in **P2** is concave. However, by applying (7), this equation is NP-hard [40]. As confirmed in the literature, the AMBM based on the KM algorithm discovers the maximum weighted matching for any given bipartite graph in all the cases. The maximum bipartite matching approach has been widely used for solving the resource allocation problem [27]–[29], [31]. However, the AMBM method cannot tackle the problem straightforwardly cause of additional constraints, i.e., C3 and C4, in this

specific problem. The AMBM method is presented in part A of Section IV, and the generalization of solving the problems is made in part B of Section IV.

A. Bipartite Maximum Weighted Matching for SCMA Asymmetric Graph

The graph of Fig. 2 can be represented by the bipartite graph $G(U, V, \varphi)$. In this bipartite graph, U and V are two sets of vertices that show FNs (RBs) and VNs (users), respectively. φ denotes the edge set of the graph. Regarding that the SCMA system mode is $\frac{|V|}{|U|} = \frac{J}{K} > 1$, G is an asymmetric bipartite graph. For a graph $G(U, V, \varphi)$, the resource assignment problem means finding a matching \bar{m} with the maximum sum of edge weights from the FN set of size K to the VN set of size J , where all the nodes (FN_k) in U are connected to J vertices (VN_j) in V , and edge (FN_k, VN_j) has the weight of R_k^j . It is worth noting that the weight of the edge is obtained by assigning FN_k to VN_j , considering a particular criterion \mathcal{R} . $\mathbf{B}_{K \times J}$ shows the matrix of values for weights of the edges. The essential criterion in the proposed method is the average sum rate of all RBs. Similar to the MO method that focuses on several objectives [41], in contrast to the traditional bipartite matching methods, two objectives, \mathcal{R}_1 and \mathcal{R}_2 from the SCMA network, are selected to find the optimal matching.

At first, the symmetric graph case with two targets \mathcal{R}_1 and \mathcal{R}_2 , is considered where the number of users and RBs are equal, i.e., $|U| = |V| = K$. The target vector of the MO problem for the bipartite matching is written as [32]

$$\mathcal{R}(\bar{m}_i) = (\mathcal{R}_1(\bar{m}_i), \mathcal{R}_2(\bar{m}_i)), \quad \bar{m}_i \in \bar{M}, \quad (21)$$

The set of all the possible states for matching is $\bar{M} = \{\bar{m}_1, \dots, \bar{m}_{K!}\}$, and the total number of possible states is $K!$ under exhaustive enumeration. The dual-objective optimization problem is converted into a single-objective optimization problem by changing the sub-key objective as the constraints of key objective. Here, \mathcal{R}_1 and \mathcal{R}_2 must be maximized through selecting the optimal matching.

The proposed algorithm has to update the graph G and \bar{m} to G' and \bar{m}' to reduce the number of possible states for the matching set \bar{M} by eliminating an edge at each iteration until no edge remains in G' . The process of updating G to G' is applied to $\mathcal{R}_1(\bar{m}_i)$ by the KM algorithm [26], which leads to a perfect matching \bar{m} with K edges. A perfect matching \bar{m} is obtained in the current iteration. In this method, one edge among all edges in \bar{m} is removed at each iteration, and the corresponding weight will set to zero to reach a trade-off between the key and sub-key objectives. KM method can conclude the maximum weighted matching for the bipartite graph as well. The KM algorithm helps to find the perfect matching for the matching set \bar{M} . For later comparisons between obtained solutions, the performance results of optimization objectives are recorded.

Given that some edges exist between node pairs from two different node sets in a complete bipartite graph, the total number of edges will be K^2 . The upper limit of iterations number is $O(K^2)$, and the maximum size of matching set M decreases to K^2 . Moreover, decision-making on removing

an edge with the minimum effect on $\mathcal{R}_1(\bar{m})$ is performed based on the performance of $\mathcal{R}_2(\bar{m})$. If the changes in the main target, $\Delta\mathcal{R}_1(\bar{m})$, are highly dependent on the changes in edge weights, then the value $\mathcal{R}_1(\bar{m})$ is calculated using the edge weights and their variations, and $\mathcal{R}_1(\bar{m})$ is updated to $\mathcal{R}_1(\bar{m}')$. In this case, the eliminated edge has less weight for the main objective. However, if changing the weights is ineffective on the performance of $\mathcal{R}_1(\bar{m}')$, i.e., $\Delta\mathcal{R}_1(\bar{m}')$ is negligible, the mentioned algorithm utilizes $\mathcal{R}_2(\bar{m}')$ for decision making. $\mathcal{R}_2(\bar{m})$ should be a criterion that $\Delta\mathcal{R}_2(\bar{m})$ depends on both the changes of the edge weights and the weights that remain unchanged during the updating \bar{m} to \bar{m}' . The objective of the proposed algorithm is to gradually improve the performance of $\mathcal{R}_2(\bar{m})$ during the process of transforming G to G' considering the maximization of the performance of $\mathcal{R}_1(\bar{m})$. Therefore, the problem is presented as follows regarding \mathcal{R}_2 as a constraint for the key objective \mathcal{R}_1 .

$$\begin{aligned} & \max \mathcal{R}_1(\bar{m}), \\ & \text{s.t. } \mathcal{R}_2(\bar{m}) \leq \epsilon, \bar{m} \in \bar{M} = \{\bar{m}_1, \dots, \bar{m}_k\}, \\ & \sum_{k=1}^K \omega_j[k] \leq 1, \forall (j, k) \in \bar{m}, \\ & \omega_j[k] \geq 0, \forall (j, k) \in \bar{m}, \end{aligned} \quad (22)$$

where ϵ is a parameter applied to \mathcal{R}_2 and helps find the best \bar{m} in the reduced set \bar{M} .

In the asymmetric graph $G(U, V, \varphi)$ of the SCMA network, $J - K$ number of zero rows are added to the original matrix of edge weights, i.e., matrix $\mathbf{B}_{K \times J}$, to form the square matrix $\mathbf{B}_{J \times J}$. $\mathbf{B}_{K \times J}$ is the individual rate matrix with entries R_k^j . Then symmetric $\mathbf{B}_{J \times J}$ is formed as shown in (23), and bipartite matching is carried out. For this purpose, matrix $\mathbf{B}_{J \times J}$ requires the initialization of matrix $\mathbf{B}_{K \times J}$, which is performed through initializing all weight elements $\omega_j[k]$.

$$\mathbf{B}_{K \times J} = \begin{bmatrix} R_1^1 & \dots & R_1^J \\ \vdots & \vdots & \vdots \\ R_k^1 & \dots & R_k^J \end{bmatrix} \rightarrow \begin{bmatrix} R_1^1 & \dots & R_1^J \\ \vdots & \vdots & \vdots \\ R_k^1 & \dots & R_k^J \\ 0 & 0 & \dots & 0 & 0 \\ 0 & 0 & \dots & 0 & 0 \end{bmatrix} = \mathbf{B}_{J \times J}. \quad (23)$$

Suppose the resource assignment process is performed by considering d_k . In that case, it is necessary to consider all possible states of selecting d_k users from J users, i.e., $\binom{J}{d_k}$. Therefore, each group of users is connected to a single RB, and the dimension of the matrix of edge weight will be $\frac{J!}{(J-d_k)!d_k!} \times \frac{J!}{(J-d_k)!d_k!}$. Considering this issue and N in the decision-making process for selecting the best matching set will increase the computation complexity. Therefore we assume all users can connect to every RB according to (23).

As we maximize the network sum rate using \mathcal{R}_1 , the users' individual rate is essential regarding their throughput requirements. For this purpose, \mathcal{R}_2 is assumed as the system fairness, which shows the users' satisfaction. Therefore, the proposed method makes an effort to maximize JFI. Similar to [32], for different edges with weight R_k^j in matching \bar{m} during the KM

process, the variation parameter $\eta_{k,j}^{\mathcal{R}_2}$ is defined as follows

$$\eta_{k,j}^{\mathcal{R}_2} = \left| R_k^j - \frac{\sum_{j=1}^J R_k^j}{J} \right|^2, \quad (24)$$

Then, the edge $b(j, k)$ that has the least effect on the performance of \mathcal{R}_2 , i.e., the change of weight in this edge provides the minimum $\Delta\mathcal{R}_2(\bar{m})$, is selected as

$$b(j, k) = \arg \max_{j,k} \left\{ \eta_{k,j}^{\mathcal{R}_2} \right\}. \quad (25)$$

It should note that if the selected least effective edges on \mathcal{R}_2 are identical, the final edge is eliminated in this iteration.

B. The Four-Step SCMA Resource Allocation

After completing the weighted bipartite matching process, resource allocation among the users and RBs is performed. According to the Section IV-A, the final derived matrix $\mathbf{B}_{K \times J}$ is used by considering d_k and N . For the proposed algorithm, since the matrix $\mathbf{B}_{K \times J}$ entries are determined based on weights of edges, the final changes of weights are also specified. The resource allocation process is implemented as follows.

1. We select the Row Maximum Entries (RMEs) in all matrix $\mathbf{B}_{K \times J}$ rows, which do not have the same columns. We fix their weight elements $\omega_j[k]$ in the AWGM, i.e., the k th row and j th column. Then, we update matrix $\mathbf{B}_{K \times J}$ by zeroing the value of rows and columns corresponding to those maximums in $\mathbf{B}_{K \times J}$. Consequently, all resources are assigned to K distinctive users, as shown in the example and the first step of Fig. 3.

2. For the remaining $J - K$ users, i.e., VN_2 and VN_5 , as shown in the example and the second step of Fig. 3, the Column Maximum Entries (CMEs) of the matrix $\mathbf{B}_{K \times J}$ are selected. If they have no identical rows, we fix their equivalent weight elements in AWGM. Next, their equivalent rows and columns in the matrix $\mathbf{B}_{K \times J}$ are set to zero. As a result, $J - K$ different RBs are assigned to the remaining $J - K$ users.

3. After applying steps 1 and 2, $2K - J$ rows with one single connection will remain in the AWGM matrix similar to FN_1 and FN_4 in Fig. 3. The maximum entries of their equivalent rows of $\mathbf{B}_{K \times J}$ are selected if there are no similar columns. We fix their weight element values in AWGM and set them zero in $\mathbf{B}_{K \times J}$.

4. After applying steps 1, 2, and 3, $J - K$ users have satisfied N connections condition similar to VN_1 and VN_2 in the third step of Fig. 3, and their equivalent columns elements are set zero in $\mathbf{B}_{K \times J}$. Columns 1 and 2 are set zero in $\mathbf{B}_{K \times J}$ like the fourth step of Fig. 3. Next, each row's maximum entries with no common columns corresponding to the remaining users similar to VN_3 , VN_4 , VN_5 , and VN_6 in the third step of Fig. 3 are selected. Then their equivalent weight elements are fixed in AWGM, and all non-fixed elements of AWGM are set equal to zero.

The Four-step resource allocation process is summarized in Algorithm 1.

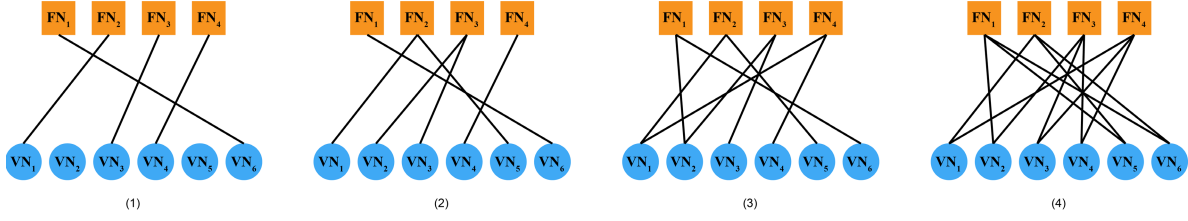


Fig. 3. Representation of the resource assignment process of algorithm 1 for SCMA.

Algorithm 1 SCMA resource allocation based on the Asymmetric Bipartite Maximum Weighted Matching

```

1: Initialize
   1:  $K$  = number of FNs,  $J$  = number of VNs,
    $N$  = number of Non-zero elements of user.
2: Obtain  $\mathbf{B}_{K \times J}$  according to Section IV-A.
3:  $\mathbf{W}(k, j) = 0$  for  $k = 1, \dots, K$  and  $j = 1, \dots, J$ .
4: for  $k = 1 : K$  do
5:   Find the RME  $b_{k,j_k}$  of the  $k$ th row of  $\mathbf{B}_{K \times J}$ .
6:   if the  $j_k$ th column with RME has the other RMEs, then
7:     set  $b_{k,j_k} = 0$ ;  $\mathbf{W}(k, j_k) = \sqrt{\omega_{j_k}[k]}$ .
8:   end if
9:   Find the RMEs in the  $j_k$ th column and set it to be 0;
   For the rest rows with RMEs in the  $j_k$ th column, set the
   maximum SRME to 0; Set the corresponding entry of  $\mathbf{W}$ 
   to  $\sqrt{\omega_{j_k}[k]}$ .
10: end for
11: for  $j \in \{\text{the remaining } (J - K) \text{ VNs without}$ 
     $\text{connections}\}$ , do
12:   Find the CMEs  $b_{k_j,j}$  of the  $(J - K)$  VNs.
13:   if the  $k_j$ th row in the  $(J - K)$  VNs has no other CMEs,
    then
14:     set  $b_{k_j,j} = 0$ ;  $\mathbf{W}(k_j, j) = \sqrt{\omega_j[k]}$ .
15:   end if
16:   Find the maximum CMEs in the  $k_j$ th row, and set it to
    be 0; For the rest columns with CMEs in the  $k_j$ th row,
    set the SCME to 0; Set the corresponding entry of  $\mathbf{W}$  to
     $\sqrt{\omega_j[k]}$ .
17: end for
18: for  $k \in \{\text{the } (2K - J) \text{ FNs with a single connection}\}$ , do
19:   (5)-(9) to the  $(2K - J)$  FNs.
20: end for
21: for  $j \in \{\text{the } (J - K) \text{ VNs with a single connection}\}$ , do
22:   (12)-(16) to the  $(J - K)$  VNs.
23: end for
24: Repeat (4)-(23) until each VN connects to  $N$  FNs, and
    each FN connects to  $JN/K$  VNs.

```

C. An Example to Demonstrate the Algorithm 1

Now we take a matrix $\mathbf{B}_{4 \times 6}$ as an example to show the resource allocation, including RB assignment and transmit power fraction allocation, that is, $K = 4$, and $J = 6$. Suppose that the entries of $\mathbf{B}_{4 \times 6}$, which is obtained from Section (IV-A), as shown in (26)

$$\mathbf{B}_{4 \times 6} = \begin{bmatrix} 1 & 5 & 1 & 2 & 4 & 9 \\ 8 & 4 & 3 & 6 & 7 & 9 \\ 8 & 6 & 9 & 2 & 3 & 3 \\ 5 & 3 & 4 & 9 & 2 & 1 \end{bmatrix}. \quad (26)$$

In algorithm 1, if we set an entry of $\mathbf{B}_{K \times J}$ to 0, we will choose the corresponding column (user) to use the corresponding row (RB) of that entry. In the algorithm, we set the maximum entry to 0 to maximize the sum rate of the SCMA network. In the example of $\mathbf{B}_{4 \times 6}$, the entries of (1, 6), (2, 6), (3, 3), and (4, 4) in (26) are RMEs with values 9. Since the 3rd and the 4th columns do not include other RMEs except from (3, 3) and (4, 4), the two entries are replaced by 0. However, the 6th column includes two RMEs (1, 6) and (2, 6) with values of 9. The entry (1, 6) is replaced by 0 because the SRME of the 1st row is smaller than the SRME of the 2nd row. Find the SRME of the 2nd row, that is, the entry (2, 1) with value 8. Since there is no RME in the 1st column, the entry (2, 1) is replaced by 0. (27) shows the results.

$$\begin{bmatrix} 1 & 5 & 1 & 2 & 4 & 9 \\ 8 & 4 & 3 & 6 & 7 & 9 \\ 8 & 6 & 9 & 2 & 3 & 3 \\ 5 & 3 & 4 & 9 & 2 & 1 \end{bmatrix} \rightarrow \begin{bmatrix} 1 & 5 & 1 & 2 & 4 & 0 \\ 0 & 4 & 3 & 6 & 7 & 9 \\ 8 & 6 & 0 & 2 & 3 & 3 \\ 5 & 3 & 4 & 0 & 2 & 1 \end{bmatrix} \triangleq \mathbf{B}_{4 \times 6}^{(1)} \quad (27)$$

In the example, column 2 and column 5 of the matrix $\mathbf{B}_{4 \times 6}^{(1)}$ form submatrix $\mathbf{B}_{4 \times 2}$, as shown in (28). The entries (3, 1) and (2, 2) are the CMEs with the values of 6 and 7. These entries are replaced by 0 since there are no CME in the 3rd and the 2nd rows. Then, the updated submatrix is put back to matrix $\mathbf{B}_{4 \times 6}^{(1)}$, and the corresponding entries of $\mathbf{B}_{4 \times 6}^{(1)}$ are replaced by the updated submatrix, as shown in (28)

$$\begin{bmatrix} 5 & 4 \\ 4 & 7 \\ 6 & 3 \\ 3 & 2 \end{bmatrix} \rightarrow \begin{bmatrix} 5 & 4 \\ 4 & 0 \\ 0 & 3 \\ 3 & 2 \end{bmatrix} \rightarrow \begin{bmatrix} 1 & 5 & 1 & 2 & 4 & 0 \\ 0 & 4 & 3 & 6 & 0 & 9 \\ 8 & 0 & 0 & 2 & 3 & 3 \\ 5 & 3 & 4 & 0 & 2 & 1 \end{bmatrix} \triangleq \mathbf{B}_{4 \times 6}^{(2)} \quad (28)$$

In the example, the 1st and 4th rows of matrix $\mathbf{B}_{4 \times 6}^{(2)}$ have only one connection to the users and form a submatrix $\mathbf{B}_{2,6}$. Applying step 1 on $\mathbf{B}_{2,6}$, and $\mathbf{B}_{2,6}$ is updated as shown in (29)

$$\begin{bmatrix} 1 & 5 & 1 & 2 & 4 & 0 \\ 5 & 3 & 4 & 0 & 2 & 1 \end{bmatrix} \rightarrow \begin{bmatrix} 1 & 0 & 1 & 2 & 4 & 0 \\ 0 & 3 & 4 & 0 & 2 & 1 \end{bmatrix}. \quad (29)$$

Put the updated submatrix $\mathbf{B}_{2,6}$ back in (29) to the matrix $\mathbf{B}_{4 \times 6}^{(2)}$ and replace the corresponding entries of $\mathbf{B}_{4 \times 6}^{(2)}$ with those of $\mathbf{B}_{2,6}$. Then, we have the updated matrix as shown in (30)

$$\mathbf{B}_{4 \times 6}^{(3)} \triangleq \begin{bmatrix} 1 & 0 & 1 & 2 & 4 & 0 \\ 0 & 4 & 3 & 6 & 0 & 9 \\ 8 & 0 & 0 & 2 & 3 & 3 \\ 0 & 3 & 4 & 0 & 2 & 1 \end{bmatrix}. \quad (30)$$

For instance, the 1st and 2nd columns of $\mathbf{B}_{4 \times 6}^{(3)}$ have two connections to the function nodes, and the rest columns only

have a single connection to the function node. Consider the submatrix $\mathbf{B}_{4 \times 4}$ formed by the 3rd, 4th, 5th, and 6th columns of $\mathbf{B}_{4 \times 6}^{(3)}$. Apply step 2 to update $\mathbf{B}_{4 \times 4}$, as shown in (31)

$$\begin{bmatrix} 1 & 2 & 4 & 0 \\ 3 & 6 & 0 & 9 \\ 0 & 2 & 3 & 3 \\ 4 & 0 & 2 & 1 \end{bmatrix} \rightarrow \begin{bmatrix} 1 & 2 & 0 & 0 \\ 3 & 6 & 0 & 0 \\ 0 & 0 & 3 & 3 \\ 0 & 0 & 2 & 1 \end{bmatrix}. \quad (31)$$

Put the updated $\mathbf{B}_{4 \times 4}$ back to $\mathbf{B}_{4 \times 6}^{(3)}$ and replace the corresponding entries of $\mathbf{B}_{4 \times 6}^{(3)}$ by those of $\mathbf{B}_{4 \times 4}$ to derive $\mathbf{B}_{4 \times 6}^{(4)}$, as shown in (32)

$$\mathbf{B}_{4 \times 6}^{(4)} \triangleq \begin{bmatrix} 1 & 0 & 1 & 2 & 0 & 0 \\ 0 & 4 & 3 & 6 & 0 & 0 \\ 8 & 0 & 0 & 0 & 3 & 3 \\ 0 & 3 & 0 & 0 & 2 & 1 \end{bmatrix}. \quad (32)$$

Repeat the steps until each user has N connections to the function nodes, and each function node has JN/K connections to the users. In the example of $\mathbf{B}_{4 \times 6}$, $N = 2$. Then, $\mathbf{B}_{4 \times 6}^{(4)}$ is the final matrix, where each user has 2 connections to the function nodes, and each function node has $(6 \times 2)/4 = 3$ connections to the users.

Finally, the entry (k, j) of \mathbf{W} is set to $\sqrt{\omega_j[k]}$ if $b_{k,j} = 0$, otherwise set it to 0. Then the fixed AWGM is expressed as

$$\mathbf{W} = \begin{bmatrix} 0 & \sqrt{\omega_2[1]} & 0 & 0 & \sqrt{\omega_5[1]} & \sqrt{\omega_6[1]} \\ \sqrt{\omega_1[2]} & 0 & 0 & 0 & \sqrt{\omega_5[2]} & \sqrt{\omega_6[2]} \\ 0 & \sqrt{\omega_2[3]} & \sqrt{\omega_3[3]} & \sqrt{\omega_4[3]} & 0 & 0 \\ \sqrt{\omega_1[4]} & 0 & \sqrt{\omega_3[4]} & \sqrt{\omega_4[4]} & 0 & 0 \end{bmatrix}. \quad (33)$$

The representation of the resource assignment process for this example is shown in Fig. 3.

It should be noted that once the AMBM process based on the individual rate of users is completed, optimal matching determines the $\mathbf{B}_{K \times J}$ matrix, as shown in (23) according to the problem targets. This matrix determines the behavior of each user with other users that have interference in each RB. Finally, using algorithm 1 helps identify AWGM.

V. SIMULATION RESULTS

This section presents the simulation results of the proposed algorithm to validate the performance improvement of the SCMA network, which is represented as AWGM. Regarding the used baseline algorithms, besides the OFDMA scheme [42], we also consider other three SCMA algorithms. The first and second ones are Max-SR and Max-Min schemes in [21], respectively, where the first one aims to maximize the average sum rate of the network while the second algorithm maximizes fairness. These methods are referred to as Max-SR-BSUM and Max-Min-BSUM. For the third one, we decompose the average sum rate maximization problem into two sub-problems: resource assignment and power allocation. Its resource assignment method is TA in [25], where a bipartite graph is generated based on users' channel and rate information. Its power allocation is the scheme of [9], which tries to find optimal solutions by the Lagrange dual method after factor graph matrix specification. This scheme is referred

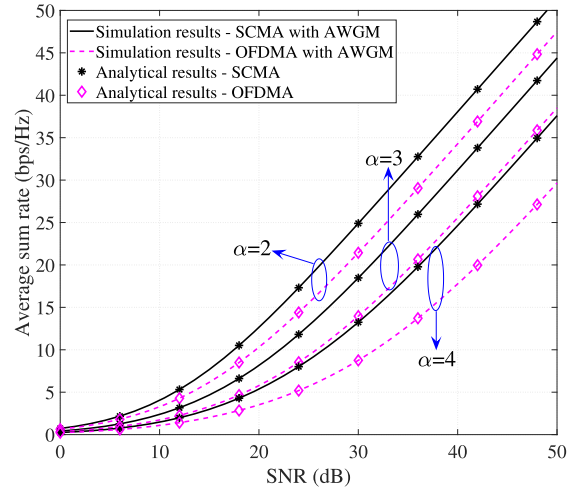


Fig. 4. Comparison of the average sum rates of SCMA and OFDMA systems with AWGM for $\alpha = 2, 3, 4$, $R_0 = 1$ m and $R_1 = 20$ m.

to as TA-PA. The solutions of [25] and [9] are not represented separately because power allocation in [25] improves EE of downlink SCMA system, and resource assignment in [9] selects the user with the maximal individual rate for each RB. In the simulations, the numbers of users and RBs are $J = 6$ and $K = 4$, respectively. The users are randomly distributed in the disk-shaped cell, with $N = 2$ and $d_f = 3$, as shown in Fig. 1.

A. SCMA Versus OFDMA With AWGM

Fig. 4 compares the average sum rate under conditions of $R_0 = 1$ m and $R_1 = 20$ m for $\alpha = 2, 3, 4$. Towards a fair comparison, the elements of AWGM for SCMA are normalized as $\sqrt{\omega_j[k] / \sum_{r=1}^K \omega_j[r]}$. Furthermore, for OFDMA, the input power is applied by a factor J/K , and the entries of AWGM for OFDMA are set equal to 1. As seen from Fig. 4, the performance of SCMA with AWGM outperforms the OFDMA with AWGM in the whole range of SNRs. Moreover, it can be observed that the average sum rate for either the SCMA system or OFDMA decreases as the path loss exponent increases. It should be noted that using AWGM in the OFDMA system significantly improves the system's performance. The reason is that according to equal numbers of OFDMA users and RBs, we can perform optimal perfect matching using the algorithm given in Section IV without algorithm part B. It can also be obtained from Fig. 4 that the simulation results match with the analytical results very well.

B. Average Sum Rate Comparison

Fig. 5 shows how the average sum rate varies with SNR for four considered algorithms. The average sum rate of the SCMA network with the Max-Min-BSUM algorithm underperforms the proposed AWGM, the Max-SR-BSUM, and the TA-PA algorithms. Fig. 5 shows that the performance of the TA-PA is worse than the AWGM and the Max-SR-BSUM methods. Because user j selects the RB k based on its maximum normalized rate in assignment for TA method, unlike

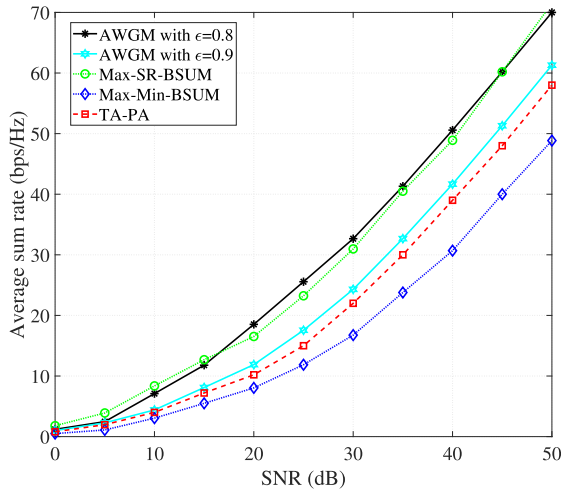


Fig. 5. Average sum rate comparison for $\alpha = 4$, $J = 6$, $K = 4$, $N = 2$, $d_k = 3$, $R_0 = 1$ m and $R_1 = 10$ m.

the PA method's objective in the TA-PA algorithm, that is the average sum rate maximization. As can be seen, the Max-SR-BSUM algorithm achieves a slightly better average sum rate than AWGM with $\epsilon = 0.9$, although the performance of AWGM with $\epsilon = 0.8$ is better than the Max-SR-BSUM method. As indicated, there is a trade-off between JFI and the average sum rate. Furthermore, our proposed algorithm's goal is the average sum rate and JFI maximization as key and sub-key objectives, respectively. Our proposed algorithm, by the edge deletion decision defined in Section IV-A, tries to keep the more critical matchings among the sets of all possible matchings. In contrast, the algorithm Max-SR-BSUM maximizes the average sum rate by achieving the locally optimal solution, which depends on initial values for power allocation and factor graph matrices. This reason is also valid for fairness maximization by Max-Min-BSUM.

C. JFI Comparison

Fig. 6 compares JFI in terms of maximum transmitted power by users. AWGM with $\epsilon = 0.8$ significantly outperforms the other algorithms, which perfectly shows its fairness. However, Max-Min-BSUM achieves a higher JFI than AWGM with $\epsilon = 0.8$, Max-SR-BSUM, and TA-PA. Moreover, Max-Min-BSUM approaches AWGM with $\epsilon = 0.9$ at a higher transmit power range. It is worth noting that Max-SR-BSUM and TA-PA algorithms are not designed to satisfy users' fairness. As a result, Fig. 6 shows that JFI for the TA-PA algorithm is lower than Max-SR-BSUM. Because the user, which is first selected based on maximum normalized rate without considering the other users' interference effect, will have a high channel gain. This algorithm helps this user select the best achievable channel gain while the user that faces weak RBs is sent to the end of the queue simultaneously. Fig. 5 and Fig. 6 show that our proposed AWGM can achieve a more balanced performance concerning the multiple objectives. While the algorithms Max-SR-BSUM, Max-Min-BSUM, and TA-PA, can not compromise the average sum rate and fairness among all users.

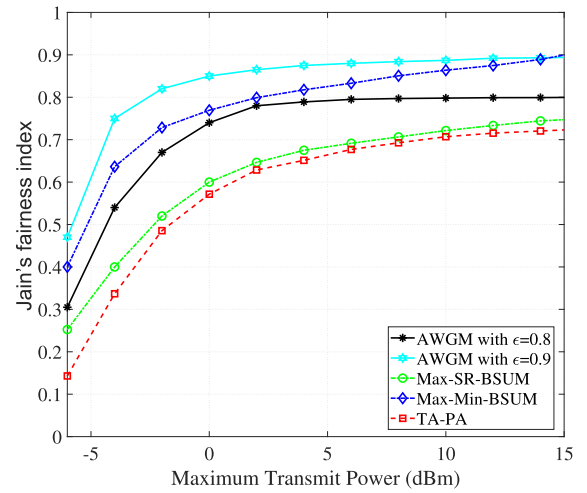


Fig. 6. JFI comparison for $\alpha = 4$, $J = 6$, $K = 4$, $N = 2$, $d_k = 3$, $R_0 = 1$ m and $R_1 = 10$ m.

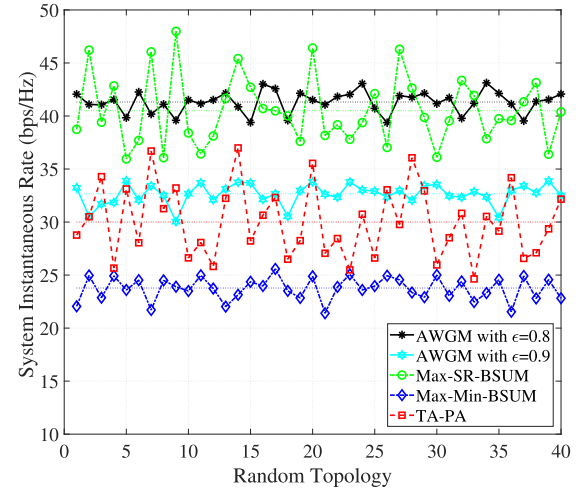


Fig. 7. System instantaneous rate variation comparison with different topologies with SNR = 35dB.

D. System Instantaneous Rate Stability

Fig. 7 depicts the instantaneous rate of the system for 40 random topologies with SNR= 35dB. Users are randomly distributed for each topology, and the effects of user interference are applied to the system instantaneous rate. The standard deviations of the AWGM with $\epsilon = 0.8$ and $\epsilon = 0.9$, Max-SR-BSUM, Max-Min-BSUM, and TA-PA are expressed as 1.02, 0.96, 3.24, 1.12, and 3.36, respectively, and this demonstrates that the instantaneous rate of Max-SR-BSUM and TA-PA algorithms varies much with different topologies. At the same time, AWGM and Max-Min-BSUM can achieve a more stable network rate because users interference effect is critical in these algorithms process. In contrast, the interference effect is not applied in Max-SR-BSUM and TA-PA algorithms. A practical wireless network needs to ensure a stable network performance where users are randomly distributed at different times, while AWGM provides it by preserving the improvement of both the average sum rate and JFI.

VI. CONCLUSION

We have proposed a new resource allocation algorithm for the uplink SCMA scheme to satisfy the objectives performance

and compromise them, where users are randomly distributed in a disk-shaped cell. For this purpose, the exact analytical expressions for the average sum rate and individual rate based on the AWGM have been derived, which simplifies our MO problem by using the AMBM approach. During the AMBM process, we have considered a power allocation strategy for improving two objective performances in the optimal resource assignment. The AWGM has been extracted for the SCMA system by using the four-step algorithm after the AMBM process. Besides the OFDMA scheme, we have compared our proposed algorithm with Max-SR, Max-Min [21], and TA-PA algorithms [9], [25]. The simulation and theoretical results have demonstrated that the performance of SCMA is superior to OFDMA, while our scheme also improves the performance of OFDMA. The results provided by the comparison with three algorithms have shown that our method by the edge deletion decision tries to keep the more crucial matchings and compromise two objectives performance while guaranteeing a stable range of network performance at different times.

APPENDIX A PROOF OF THEOREM 1

Note that the auto-correlation matrix $\mathbf{E}\{\mathbf{X}_j\mathbf{X}_j^H\} = \text{diag}(\omega_j[1], \dots, \omega_j[K])$ is diagonal. Using [35, eq. (2.15)], [36, eq. (4)] and applying $\det(\cdot)$, (6) is written as follows

$$\sum_{j=1}^J R^j \leq \mathbf{E}_h \left\{ \log \prod_{k=1}^K \left(1 + \frac{E_t}{N} \sum_{j=1}^J \left(g_j[k] d_j^{-\frac{\alpha}{2}} \right)^2 \omega_j[k] \right) \right\}. \quad (34)$$

Since two independent random variables form $h_j[k]$, their multiplication inside the logarithmic function is expressed by a summation form as follows

$$\sum_{j=1}^J R^j \leq \mathbf{E}_h \left\{ \sum_{k=1}^K \log \left(1 + \frac{E_t}{N} \sum_{j=1}^J \left(\omega_j[k] |g_j[k]|^2 d_j^{-\alpha} \right) \right) \right\}. \quad (35)$$

By using the upper bound for the average sum rate, the proof is completed.

APPENDIX B PROOF OF THEOREM 2

It should note that, for the calculation of \mathcal{L}_{μ_j} , the PDF of link distance, cell shape, and $f_{V_j}(v)$ entirely differ from those given in [22]. For the current scenario, \mathcal{L}_{μ_j} is expressed as

$$\mathcal{L}_{\mu_j} \left(s \frac{E_t}{N} \right) = \frac{2}{R_1^2 - R_0^2} \times \int_{R_0}^{R_1} x^{\alpha+1} \left(\int_0^\infty e^{-\frac{sE_t}{N}\mu_j} f_{V_j}(x^\alpha \mu) d\mu \right) dx. \quad (36)$$

Combining (10) and (36), the integral is solved in terms of μ_j as

$$\mathcal{L}_{\mu_j} \left(s \frac{E_t}{N} \right) = \frac{2}{R_1^2 - R_0^2} \int_{R_0}^{R_1} \frac{x^{\alpha+1}}{s \frac{E_t \omega_j[k]}{N} + x^\alpha} dx. \quad (37)$$

Using the integral form of hyper-geometric functions [38, eq. (15.3.1)], we have

$$\begin{aligned} \mathcal{L}_{\mu_j} \left(s \frac{E_t}{N} \right) &= \frac{2}{R_1^2 - R_0^2} \\ &\times \frac{N}{s E_t \omega_j[k] (\alpha + 2)} \times \left(x^{\alpha+2} H \left(\frac{-N x^\alpha}{s E_t \omega_j[k]} \right) \Big|_{R_0}^{R_1} \right), \end{aligned} \quad (38)$$

where

$$\begin{aligned} \tilde{H} \left(\frac{-N x^\alpha}{s E_t \omega_j[k]} \right) &= {}_2F_1 \left(1, 1 + \frac{2}{\alpha}, 2 + \frac{2}{\alpha}, - \left(\frac{N}{s E_t \omega_j[k]} \right) x^\alpha \right), \end{aligned} \quad (39)$$

${}_2F_1$ is called the generalized hyper-geometric function, which is a particular form of the hyper-geometric function [38, eq. (15.1.1)]. (39) is used for simplicity. Substituting (38) into (8), the proof is completed.

APPENDIX C PROOF OF THEOREM 3

According to (7), the sum rate of all users is equal to the sum achievable rate from all the RBs, i.e.,

$$\sum_{j=1}^J R^j \approx \sum_{k=1}^K R_k, \quad (40)$$

where the achievable rate R_k at RB k is

$$R_k = \mathbf{E} \left\{ \log \left(1 + \frac{E_t}{N} \sum_{j=1}^J \omega_j[k] |g_j[k]|^2 d_j^{-\alpha} \right) \right\}. \quad (41)$$

In a connection between a user and an RB, only one non-zero element is allocated to the RB. Hence, using the specifications of the logarithmic relationship $\log(a + b) = \log(a) + \log(1 + \frac{b}{a})$, (41) is expressed as (42), given at the top of the next page.

In the above derivations, it is assumed that the remaining $J - 1$ users play the role of interference for the j th user. The algorithm process of Section IV with d_k and N constraints leads to satisfying the problem targets. The achievable rate R_k at each RB is equal to the summation of users individual rates assigned to that RB, i.e., $R_k = \sum_{j=1}^J R_k^j$, where R_k^j is obtained by

$$R_k^j = \mathbf{E} \left\{ \log \left(\frac{\omega_j[k] |g_j[k]|^2 d_j^{-\alpha}}{\frac{N}{E_t} + \sum_{\substack{t=1 \\ t \neq j}}^J \omega_t[k] |g_t[k]|^2 d_t^{-\alpha}} \right) \right\}, \quad (43)$$

$$\begin{aligned}
R_k &= \mathbf{E} \left\{ \log \left(1 + \frac{E_t}{N} \omega_1[k] |g_1[k]|^2 d_1^{-\alpha} \right) + \log \left(\frac{(1 + \frac{E_t}{N}) (\omega_1[k] |g_1[k]|^2 d_1^{-\alpha} + \omega_2[k] |g_2[k]|^2 d_2^{-\alpha})}{1 + \frac{E_t}{N} \omega_1[k] |g_1[k]|^2 d_1^{-\alpha}} \right) + \dots \right. \\
&\quad \left. + \log \left(\frac{1 + \frac{E_t}{N} \sum_{t \neq j}^J \omega_t[k] |g_t[k]|^2 d_t^{-\alpha} + \frac{E_t}{N} \omega_J[k] |g_J[k]|^2 d_J^{-\alpha}}{1 + \frac{E_t}{N} \sum_{t \neq j}^J \omega_t[k] |g_t[k]|^2 d_t^{-\alpha}} \right) \right\} \\
&= \sum_{j=1}^J \mathbf{E} \left\{ \log \left(1 + \frac{\frac{E_t}{N} \omega_j[k] |g_j[k]|^2 d_j^{-\alpha}}{1 + \frac{E_t}{N} \sum_{t \neq j}^J \omega_t[k] |g_t[k]|^2 d_t^{-\alpha}} \right) \right\} \\
&= \sum_{j=1}^J \mathbf{E} \left\{ \log \left(1 + \frac{\omega_j[k] |g_j[k]|^2 d_j^{-\alpha}}{\frac{N}{E_t} + \sum_{t \neq j}^J \omega_t[k] |g_t[k]|^2 d_t^{-\alpha}} \right) \right\}. \tag{42}
\end{aligned}$$

where the normalization of the noise variance, σ_n is assumed for simplifications, the normalized form of $\frac{N\sigma_n}{E_t}$ is used in (43) as $\frac{N}{E_t}$. In addition, neglect power of noise term compared to the interference power term in (43), i.e.,

$$\frac{N}{E_t} + \sum_{\substack{t=1 \\ t \neq j}}^J \omega_t[k] |g_t[k]|^2 d_t^{-\alpha} \approx \sum_{\substack{t=1 \\ t \neq j}}^J \omega_t[k] |g_t[k]|^2 d_t^{-\alpha}.$$

The proof is completed.

REFERENCES

- [1] M. Imran, Y. Sambo, and Q. Abbasi, *Enabling 5G Communication Systems to Support Vertical Industries*. Hoboken, NJ, USA: Wiley, Aug. 2019, pp. 253–256.
- [2] P. Pirinen, “A brief overview of 5G research activities,” in *Proc. 1st IEEE Int. Conf. 5G Ubiquitous Connectivity (5GU)*, Nov. 2014, pp. 17–22.
- [3] F. Wei, W. Chen, Y. Wu, J. Li, and Y. Luo, “Toward 5G wireless interface technology: Enabling nonorthogonal multiple access in the sparse code domain,” *IEEE Veh. Technol. Mag.*, vol. 13, no. 4, pp. 18–27, Dec. 2018.
- [4] J. Shen, W. Chen, F. Wei, and Y. Wu, “ACK feedback based UE-to-CTU mapping rule for SCMA uplink grant-free transmission,” in *Proc. 9th Int. Conf. Wireless Commun. Signal Process. (WCSP)*, Nanjing, China, Oct. 2017, pp. 1–6.
- [5] H. Nikopour and H. Baligh, “Sparse code multiple access,” in *Proc. IEEE 24th Annu. Int. Symp. Pers., Indoor, Mobile Radio Commun.*, Sep. 2013, pp. 332–336.
- [6] M. Taherzadeh, H. Nikopour, A. Bayesteh, and H. Baligh, “SCMA codebook design,” in *Proc. IEEE Veh. Technol. Conf.*, Las Vegas, NV, USA, Sep. 2014, pp. 1–5.
- [7] L. Yang, Y. Liu, and Y. Siu, “Low complexity message passing algorithm for SCMA system,” *IEEE Commun. Lett.*, vol. 20, no. 12, pp. 2466–2469, Dec. 2016.
- [8] K. Xiao, B. Xiao, S. Zhang, Z. Chen, and B. Xia, “Simplified multiuser detection for SCMA with sum-product algorithm,” in *Proc. Int. Conf. Wireless Commun. Signal Process. (WCSP)*, Nanjing, China, Oct. 2015, pp. 1–5.
- [9] Z. Li, W. Chen, F. Wei, F. Wang, X. Xu, and Y. Chen, “Joint codebook assignment and power allocation for SCMA based on capacity with Gaussian input,” in *Proc. IEEE/CIC Int. Conf. Commun. China (ICCC)*, Chengdu, China, Jul. 2016, pp. 1–6.
- [10] C. Zhong, K. Niu, J. Dai, and C. Dong, “A novel SCMA codebook construction based on extended factor graph design,” in *Proc. IEEE Globecom Workshops (GC Wkshps)*, Abu Dhabi, United Arab Emirates, Dec. 2018, pp. 1–6.
- [11] C. Yang, S. Jing, X. Liang, Z. Zhang, X. You, and C. Zhang, “A large scale extension of sparse code multiple access system,” in *Proc. IEEE Global Conf. Signal*, Nov. 2018, pp. 848–852.
- [12] X. Ma, L. Yang, Z. Chen, and Y. Siu, “Low complexity detection based on dynamic factor graph for SCMA systems,” *IEEE Commun. Lett.*, vol. 21, no. 12, pp. 2666–2669, Dec. 2017.
- [13] Y. Zheng, J. Cui, X. Lei, Z. Ding, P. Fan, and D. Chen, “Impact of factor graph on average sum rate for uplink sparse code multiple access systems,” *IEEE Access*, vol. 4, no. 99, pp. 6585–6590, Oct. 2016.
- [14] J. Bao, Z. Ma, Z. Ding, G. K. Karagiannidis, and Z. Zhu, “On the design of multiuser codebooks for uplink SCMA systems,” *IEEE Commun. Lett.*, vol. 20, no. 10, pp. 1920–1923, Oct. 2016.
- [15] L. Li, Z. Ma, P. Z. Fan, and L. Hanzo, “High-dimensional codebook design for the SCMA down link,” *IEEE Trans. Veh. Technol.*, vol. 67, no. 10, pp. 10118–10122, Oct. 2018.
- [16] S. Zhang *et al.*, “A capacity-based codebook design method for sparse code multiple access systems,” in *Proc. 8th Int. Conf. Wireless Commun. Signal Process. (WCSP)*, Yangzhou, China, Oct. 2016, pp. 1–5.
- [17] D. Zhai, M. Sheng, X. Wang, Y. Li, J. Song, and J. Li, “Rate and energy maximization in SCMA networks with wireless information and power transfer,” *IEEE Commun. Lett.*, vol. 20, no. 2, pp. 360–363, Feb. 2016.
- [18] Y. Zhang, X. Wang, D. Wang, Y. Zhang, and Y. Lan, “Capacity analysis and resource allocation of layered multicast in SCMA networks,” in *Proc. IEEE Wireless Commun. Netw. Conf. (WCNC)*, Barcelona, Spain, Apr. 2018, pp. 1–6.
- [19] S. Han, Y. Huang, W. Meng, C. Li, N. Xu, and D. Chen, “Optimal power allocation for SCMA downlink systems based on maximum capacity,” *IEEE Trans. Commun.*, vol. 67, no. 2, pp. 1480–1489, Feb. 2019.
- [20] J. Chen, Z. Wang, W. Xiang, and S. Yongchen, “Outage probability region and optimal power allocation for uplink SCMA systems,” *IEEE Trans. Commun.*, vol. 66, no. 10, pp. 4965–4980, Oct. 2018.
- [21] J. V. C. Evangelista, Z. Sattar, G. Kaddoum, and A. Chaaban, “Fairness and sum-rate maximization via joint subcarrier and power allocation in uplink SCMA transmission,” *IEEE Trans. Wireless Commun.*, vol. 18, no. 12, pp. 5855–5867, Dec. 2019.
- [22] Z. Yang, X. Lei, Z. Ding, P. Fan, and G. K. Karagiannidis, “On the uplink sum rate of SCMA system with randomly deployed users,” *IEEE Wireless Commun. Lett.*, vol. 6, no. 3, pp. 338–341, Jun. 2017.
- [23] L. Liu, M. Sheng, J. Liu, X. Wang, and J. Li, “Success probability and area spectral efficiency in SCMA wireless networks,” *IEEE Trans. Veh. Technol.*, vol. 67, no. 8, pp. 7764–7768, Aug. 2018.
- [24] J. Bao, Z. Ma, M. Xiao, Z. Ding, and Z. Zhu, “Performance analysis of uplink SCMA with receiver diversity and randomly deployed users,” *IEEE Trans. Veh. Technol.*, vol. 67, no. 3, pp. 2792–2797, Mar. 2018.
- [25] L. Ferdouse, S. Erkucuk, A. Anpalagan, and I. Woungang, “Energy efficient SCMA supported downlink cloud-RANs for 5G networks,” *IEEE Access*, vol. 8, pp. 1416–1430, Dec. 2020.
- [26] J. Munkres, “Algorithms for the assignment and transportation problems,” *J. Soc. for Ind. Appl. Math.*, vol. 5, no. 1, pp. 32–38, Mar. 1957.
- [27] X. Zhou, L. Yang, and D. Yuan, “Bipartite matching based user grouping for grouped OFDM-IDMA,” *IEEE Trans. Wireless Commun.*, vol. 12, no. 10, pp. 5248–5257, Oct. 2013.
- [28] L. Wang, H. Tang, H. Wu, and G. L. Stüber, “Resource allocation for D2D communications underlay in Rayleigh fading channels,” *IEEE Trans. Veh. Technol.*, vol. 66, no. 2, pp. 1159–1170, Feb. 2017.
- [29] M. Y. Hassan, F. Hussain, M. S. Hossen, S. Choudhury, and M. M. Alam, “Interference minimization in D2D communication underlaying cellular networks,” *IEEE Access*, vol. 5, pp. 22471–22484, Oct. 2017.
- [30] H. Han, Y. Li, and X. Guo, “A graph-based random access protocol for crowded massive MIMO systems,” *IEEE Trans. Wireless Commun.*, vol. 16, no. 11, pp. 7348–7361, Nov. 2017.

- [31] H. M. Kim, H. V. Nguyen, G.-M. Kang, Y. Shin, and O.-S. Shin, "Device-to-device communications underlying an uplink SCMA system," *IEEE Access*, vol. 7, pp. 21756–21768, Feb. 2019.
- [32] F. Sun, V. O. K. Li, and Z. Diao, "Modified bipartite matching for multiobjective optimization: Application to antenna assignments in MIMO systems," *IEEE Trans. Wireless Commun.*, vol. 8, no. 3, pp. 1349–1355, Mar. 2009.
- [33] K. A. Hamdi, "A useful lemma for capacity analysis of fading interference channels," *IEEE Trans. Commun.*, vol. 58, no. 2, pp. 411–416, Feb. 2010.
- [34] I. Krikidis, "Simultaneous information and energy transfer in large-scale networks with/without relaying," *IEEE Trans. Commun.*, vol. 62, no. 3, pp. 900–912, Mar. 2014.
- [35] N. Jindal, "Multi-user communication systems: Capacity, duality, and cooperation," Ph.D. dissertation, Dept. Electr. Eng. Stanford Univ., Stanford, CA, USA, Jul. 2004.
- [36] R. Razavi, R. Hoshyar, M. A. Imran, and Y. Wang, "Information theoretic analysis of LDS scheme," *IEEE Commun. Lett.*, vol. 15, no. 8, pp. 798–800, Aug. 2011.
- [37] K. A. Hamdi, "Capacity of MRC on correlated rician fading channels," *AEU-Int. J. Electron. Commun.*, vol. 56, no. 5, pp. 708–711, May 2008.
- [38] M. Abramowitz and I. A. Stegun, *Handbook of Mathematical Functions: With Formulas, Graphs, and Mathematical Tables*, vol. 55. New York, NY, USA: Dover, Oct. 1965, p. 361.
- [39] R. Jain, A. Durrees, and G. Babic, "Throughput fairness index: An explanation," *ATM Forum Contribution*, vol. 99, no. 45, Jan. 1999. [Online]. Available: <https://www.cse.wustl.edu/~jain/atmf/ftp/atm99-0045.pdf>
- [40] S. Burer and A. N. Letchford, "Non-convex mixed-integer nonlinear programming: A survey," *Surv. Oper. Res. Manage. Sci.*, vol. 17, no. 2, pp. 97–106, Jul. 2012.
- [41] E. Bjornson, E. A. Jorswieck, M. Debbah, and B. Ottersten, "Multiobjective signal processing optimization: The way to balance conflicting metrics in 5G systems," *IEEE Signal Process. Mag.*, vol. 31, no. 6, pp. 14–23, Nov. 2014.
- [42] Q. Wu, W. Chen, M. Tao, J. Li, H. Tang, and J. Wu, "Resource allocation for joint transmitter and receiver energy efficiency maximization in downlink OFDMA systems," *IEEE Trans. Commun.*, vol. 63, no. 2, pp. 416–430, Feb. 2015.



Maryam Cheraghy received the B.Eng. degree in electronic engineering from the Sadjad University of Technology in 2009 and the M.Eng. degree in communication and information systems from the Huazhong University of Science and Technology of China in 2014. She is currently pursuing the Ph.D. degree with the Department of Electronic Engineering, Shanghai Institute for Advanced Communication and Data Science, Shanghai Jiao Tong University, China. Her research interest includes wireless communication with a focus on sparse code multiple access.



Wen Chen (Senior Member, IEEE) is currently a tenured Professor with the Department of Electronic Engineering, Shanghai Jiao Tong University, China, where he is also the Director of the Broadband Access Network Laboratory. His research interests include multiple access, coded cooperation, and green heterogeneous networks. He has published 102 articles in IEEE journals and more than 120 papers in IEEE Conferences, with citations more than 6000 in Google scholar. He is a fellow of the Chinese Institute of Electronics and the distinguished lecturers of IEEE Communications Society and IEEE Vehicular Technology Society. He is the Shanghai Chapter Chair of IEEE Vehicular Technology Society, an Editors of IEEE TRANSACTIONS ON WIRELESS COMMUNICATIONS, IEEE TRANSACTIONS ON COMMUNICATIONS, IEEE ACCESS, and IEEE OPEN JOURNAL OF VEHICULAR TECHNOLOGY.



Hongying Tang (Member, IEEE) received the Ph.D. degree from Shanghai Jiao Tong University (SJTU), China, in 2015. She is currently a Senior Engineer with the Science and Technology on Microsystem Laboratory, Shanghai Institute of Microsystem and Information Technology, Chinese Academy of Sciences. Her research interests include unmanned aerial vehicle (UAV) communications and wireless sensor networks.



Qingqing Wu (Member, IEEE) received the B.Eng. degree in electronic engineering from the South China University of Technology in 2012 and the Ph.D. degree in electronic engineering Shanghai Jiao Tong University (SJTU) in 2016.

From 2016 to 2020, he was a Research Fellow with the Department of Electrical and Computer Engineering, National University of Singapore. He is currently an Assistant Professor with the State Key Laboratory of Internet of Things for Smart City, University of Macau. His current research interest

includes intelligent reflecting surface (IRS), unmanned aerial vehicle (UAV) communications, and MIMO transceiver design. He is listed as a World's Top 2% Scientist by Stanford University in 2020. He was a recipient of the IEEE WCSP Best Paper Award in 2015, the Outstanding Ph.D. Thesis Funding in SJTU in 2016, and the Outstanding Ph.D. Thesis Award of China Institute of Communications in 2017. He was the Exemplary Editor of IEEE COMMUNICATIONS LETTERS in 2019 and the Exemplary Reviewer of several IEEE journals. He serves as an Associate Editor for IEEE COMMUNICATIONS LETTERS, IEEE OPEN JOURNAL OF COMMUNICATIONS SOCIETY, and IEEE OPEN JOURNAL OF VEHICULAR TECHNOLOGY. He is the Lead Guest Editor of IEEE JOURNAL ON SELECTED AREAS IN COMMUNICATIONS on UAV Communications in 5G and Beyond Networks and the Guest Editor of IEEE OPEN JOURNAL ON VEHICULAR TECHNOLOGY on 6G Intelligent Communications and IEEE OPEN JOURNAL OF COMMUNICATIONS SOCIETY on Reconfigurable Intelligent Surface-Based Communications for 6G Wireless Networks. He is the workshop Co-Chair of IEEE ICC 2019–2021 workshop on Integrating UAVs into 5G and Beyond and the workshop Co-Chair of IEEE GLOBECOM 2020 workshop on Reconfigurable Intelligent Surfaces for Wireless Communication for Beyond 5G. He serves as the Workshops and Symposia Officer for Reconfigurable Intelligent Surfaces Emerging Technology Initiative and the Research Blog Officer for Aerial Communications Emerging Technology Initiative.



Jun Li (Senior Member, IEEE) received the Ph.D. degree in electronic engineering from Shanghai Jiao Tong University, Shanghai, China, in 2009. From January 2009 to June 2009, he worked with the Department of Research and Innovation, Alcatel Lucent Shanghai Bell as a Research Scientist. From June 2009 to April 2012, he was a Post-Doctoral Fellow with the School of Electrical Engineering and Telecommunications, The University of New South Wales, Sydney, NSW, Australia. From April 2012 to June 2015, he was a Research Fellow with the School of Electrical Engineering, The University of Sydney, Sydney, NSW, Australia. Since June 2015, he has been a Professor with the School of Electronic and Optical Engineering, Nanjing University of Science and Technology, Nanjing, China. He was a Visiting Professor with Princeton University from 2018 to 2019. He has coauthored more than 200 papers in IEEE journals and conferences, and holds one U.S. patents and more than ten Chinese patents in these areas. His research interests include network information theory, game theory, distributed intelligence, multiple agent reinforcement learning, and their applications in ultra-dense wireless networks, mobile edge computing, network privacy and security, and the Industrial Internet of Things. He was serving as an Editor of IEEE COMMUNICATION LETTERS and a TPC member for several flagship IEEE conferences. He received Exemplary Reviewer of IEEE TRANSACTIONS ON COMMUNICATIONS in 2018 and the Best Paper Award from IEEE International Conference on 5G for Future Wireless Networks in 2017.